ELSEVIER

Chemical Engineering Journal 138 (2008) 155–165

Chemical Engineering Journal

www.elsevier.com/locate/cej

Development of surface porosity and catalytic activity in metal sludge/waste oil derived adsorbents: Effect of heat treatment

Karifala Kante [a], Jieshan Qiu [b], Zongbin Zhao [b], Yu Cheng [b], Teresa J. Bandosz [a,b,*]

[a] *Department of Chemistry, The City College of New York, 138th Street and Convent Avenue, New York, NY 10031, USA*
[b] *Carbon Research Laboratory, School of Chemical Engineering, Dalian University of Technology, 158 Zhongshan Road, Dalian 116012, China*

Received 31 January 2007; received in revised form 5 June 2007; accepted 14 June 2007

Abstract

New materials were prepared by pyrolysis of metal sludge from galvanization industry saturated with spent mineral oil. To evaluate the changes in the structural and chemical properties, the pyrolysis time and temperature varied. The materials were characterized using adsorption of nitrogen, FTIR, XRD, XRF, ICP, SEM and thermal analysis. Their catalytic activity was tested in the removal of hydrogen sulfide from simulated mixture of digester gas. The results indicated that a new carbon phase from the oil precursor not only provided microporosity but also contributed to the changes in surface chemistry of the materials, which are favorable for hydrogen sulfide oxidation to elemental sulfur. Based on surface chemistry analyses the catalytic centers consist of nitrogen-containing catalytic carbon and/or spinel-like structures containing iron, zinc and nickel. Longer carbonization time and higher temperature besides bringing more stability to the carbon phase via increasing its degree of aromatization and via rearrangement in nitrogen chemistry also impose favorable changes in an inorganic phase via solid-state reactions.

Keywords: Metal sludge; Pyrolysis; Porosity; Surface chemistry; Catalytic activity

1. Introduction

Utilization of industrial wastes and their environmental "neutralization" is one of the current directions related to the environmental protection and environmental remediation [1]. One of the wastes produced in substantial quantity by heavy industry are metal sludges with different levels of environmentally hazardous components. If a valuable metal content is low and thus its recovery is not economically feasible, such sludges are usually disposed by burying big containers underground in especially designated areas. Then the metal leaching must be monitored. Although to decrease their volume and to eliminate metal leaching thermal treatment of such wastes has been proposed [2], no indication of other beneficial usage was suggested.

One of the methods to utilize sludges and other industrial and municipal wastes is their conversion into adsorbents [3–25]. Usually it is done by heat treatment at elevated temperatures. Even though simple treatment of sludge of a specific composition can lead to efficient adsorbents, chemical treatment [10] such as acid washing [14], or physical activation with steam or CO_2 [24,25] are sometimes applied. Since a low pore volume of this kind of adsorbents can be a limiting factor for their applications, to improve porosity mixtures of sludges with activated carbon or carbonaceous phase precursors such as polymers, waste oil, or waste paper were proposed [16,21–23].

In spite of the low porosity, sludge derived adsorbents were found to be competitive to activated carbons in such applications as removal of dyes [19,20], heavy metals [17–19], or sulfur containing gases [13–16]. Especially in the latter applications high capacities were reported [25–29]. The good performance of sludge derived material in desulfurization of air [26–28] or digester gas [29] was linked to the catalytic effects of their surface. Their surface chemistry is complex and various spinel-like crystalline phases formed during solid-state reactions based on iron, calcium, zinc and copper were proposed as enhancing

* Corresponding author at: Department of Chemistry, The City College of New York, 138th Street and Convent Avenue, New York, NY 10031, USA. Tel.: +1 212 650 6017; fax: +1 212 650 6107.
E-mail address: tbandosz@ccny.cuny.edu (T.J. Bandosz).

1385-8947/$ – see front matter © 2007 Elsevier B.V. All rights reserved.
doi:10.1016/j.cej.2007.06.010

the oxidation process. On the surface of this kind of materials hydrogen sulfide is predominantly oxidized to sulfur, which is important from the point of view of waste disposal or regeneration. Moreover, these kinds of catalytic centers are not easily deactivated by carbonic acid when hydrogen sulfide is removed from digester gas. Conventional carbon-based desulfurization catalyst such as DarcoH_2S® or Midas® were shown as nonefficient media for digester gas applications due to the reactivity of their CaO/MgO based catalytic phases with carbon dioxide [30].

The objective of this paper is to study the effect of mineral oil addition on the development of porous and catalytic properties of metal sludge based adsorbents. The predominant metals in the sludge are zinc, calcium and iron. They are known from their catalytic activity in retention/oxidation of hydrogen sulfide. Waste oil is expected to derive carbonaceous phase, which, besides bringing additional porosity, will take part in the solid-state reactions via providing carbon element and reducing environment. It is expected that changing the pyrolysis conditions, such as holding time and temperature, should have an effect on the extent of these reactions, on the aromatization level of an organic phase, and on the development of porosity. All of these should affect the reactive adsorption of hydrogen sulfide in the presence of carbon dioxide and methane.

2. Experimental

2.1. Materials

The adsorbents were prepared from metal sludge from General Galvanizing, Bronx, NY and spent car oil mixture. First the sludge was dried, crushed and sieved to 1–2 mm in size. The particles of dry sludge were mixed with the spent car oil (~5.5 g sludge/mL of oil). The materials were left at this stage for 1–3 days and then the pyrolysis was done. In all cases the pyrolysis was carried out at horizontal furnace at a nitrogen atmosphere with heating rate 10 °C/min. The final pyrolysis temperatures were 650 and 950 °C with holding time 30, 60 or 120 min. The adsorbents are referred to as CTO. The name is followed by the numbers representing holding time and heating temperature, respectively. Thus the CTO-30-950 represents the adsorbent derived from metal sludge saturated with oil, which was heated at 950 °C for 30 min. The names of adsorbents, their compositions and yields are collected in Table 1. For the sake of comparison, the samples obtained without oil are referred to as CT. The initial samples, without pyrolysis are denoted as T and TO.

Table 1
Yields of adsorbents, ash contents and the pH values for the initial and exhausted samples

	Yield (%)	Ash content (%)	pH initial	pH ED
CT-30-650	78	–	9.34	9.09
CT-30-950	67	–	9.91	10.94
CTO-30-650	47	76.1	10.18	9.88
CTO-60-650	47	76.0	10.48	10.10
CTO-120-650	46	76.5	9.47	9.43
CTO-30-950	42	84.0	10.63	10.21
CTO-60-950	43	85.5	10.39	10.44
CTO-120-950	43	85.0	11.30	11.13

2.2. Methods

2.2.1. Characterization of pore structure of adsorbents

On the materials obtained sorption of nitrogen at its boiling point was carried out using ASAP 2010 (Micromeritics). Before the experiments, the samples were outgassed at 120 °C (the exhausted samples were outgassed at 100 °C to minimized vaporization of elemental sulfur and weakly bonded sulfuric acid) to constant vacuum (10^{-4} Torr). From the isotherms, the surface areas (BET method), total pore volumes, V_t (from the last point of isotherm at relative pressure equal to 0.99), volumes of micropores, V_{mic} (DR [31]), mesopore volume V_{mes}, along with pore size distributions were calculated (DFT [32,33]).

2.2.2. Thermal analysis

Thermal analysis was carried out using TA instrument thermal analyzer. The instrument settings were: heating rate 10 °C/min and a nitrogen atmosphere with 100 mL/min flow rate. For each measurement about 25 mg of a ground adsorbent sample were used. From the weight loss curve the differential weight loss was calculated where peaks represent the weight loss. The ash content is listed in Table 1 as mass left after heating at 800 °C in air.

2.2.3. Surface pH

The pH of a carbonaceous sample suspension provides information about the acidity and basicity of the surface. A sample of 0.4 g of dry adsorbent powder was added to 20 mL of distilled water and the suspension was stirred overnight to reach equilibrium. Then the pH of suspension was measured.

2.2.4. XRF

To determine qualitatively the content of metals XRF experiments were carried out. For this purpose, SPECTRO Model 300T Benchtop Multi-Channel Analyzer from ASOMA Instruments, Inc. was used. It contains a titanium (Ti) target X-ray tube with Mo-2mil filter and high resolution detector with a filter. A home developed methods were selected to identify the sulfur and acquisition conditions were the following: voltage 9.0 kV, current 280 μA, count time 100 s, warm-up 3 min. Instrument reference temperature was 293 K and background conditions: lower ROI 3200, upper ROI 5750 keV.

2.2.5. Elemental analysis

The content of carbon, nitrogen and hydrogen in the samples was determined using a Vario EL III analyzer (Germany, Elementar). For the ICP analysis, the samples were calcined at 800 °C for 2 h and then dissolved in hydrochloric acid (6.0 M). The content of metals in all samples was analyzed by coupled plasma optical emission spectroscopy (ICP-OES) on Perkin-Elmer, Optima 2000DV (pump rate 1.5 mL/min, power 1300 W).

2.2.6. SEM

The analysis was carried out using A JEOL JSM-5600LV microscope. The samples were directly mounted to the sample holder with a piece of electrically conductive glue.

2.2.7. FTIR

FTIR spectra for all the samples were recorded using JASCO FT/IR-430 spectrometer with a resolution of 4 cm^{-1} (KBr pellet, carbon loading of *ca.* 0.5 wt%).

2.2.8. XRD

The crystal components of the samples were analyzed by X-ray diffraction (XRD, Rigaku D/MAX2400, Cu Kα, 40 kV and 100 mA).

2.2.9. Evaluation of H_2S sorption capacity

A custom-designed dynamic test was used to evaluate the performance of adsorbents for H_2S adsorption from gas streams as described in the technical literature [29]. Adsorbent samples were ground (1–2 mm particle size) and packed into a glass column (length 370 mm, internal diameter 9 mm, bed volume 3 cm^3). Digester gas mixture (60% CH_4, 40% CO_2) containing 0.1% (1000 ppm) of H_2S was passed through the column of adsorbent at 0.100 L/min. The flow rate was controlled using Cole Palmer flow meters. The breakthrough of H_2S was monitored using electrochemical sensors. As a breakthrough concentration 100 ppm was arbitrary chosen. The adsorption capacities of each sorbent in terms of milligram of sulfur containing gases per gram of adsorbent were calculated by integration of the area above the breakthrough curves, and from the H_2S concentration in the inlet gas, flow rate, breakthrough time and mass of the sorbent. The experiments were run on dry samples.

3. Results and discussion

The DTG curves for the initial sludge, waste oil and their sludge/oil mixture are presented in Fig. 1. The peaks represent the weight loss occurring at certain temperature ranges. As seen, introduction of oil significantly changes the metal sludge carbonization pattern. A significant mass is lost in the temperature range 200–500 °C due to the removal of volatile species from oil as a result of its decomposition and carbonization of its organic compounds. As seen on DTG curves for metal sludge containing samples, a small mass is lost at about 650 °C, likely as a result of changes in the composition/decomposition of inorganic phases. To study the effects of samples' surface chemistries on the desulfurization of digester gas, which represents here the catalytic activity, and thus to impose different surface chemistries, 650 and 950 °C were chosen as carbonization temperatures, based on the weight loss patterns.

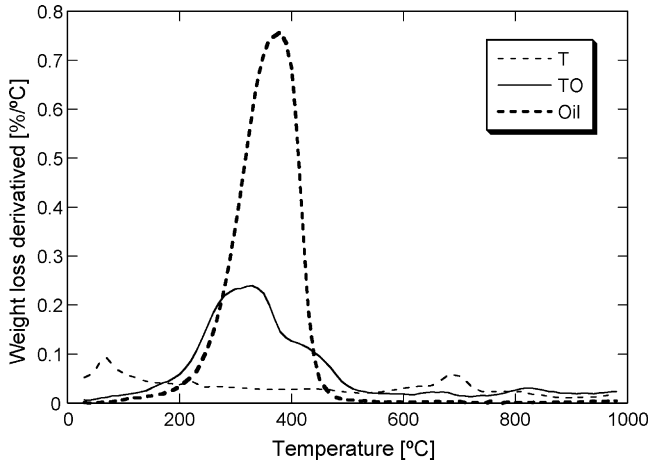

Fig. 1. DTG curves in nitrogen for the initial sludge/oil mixtures and the individual components.

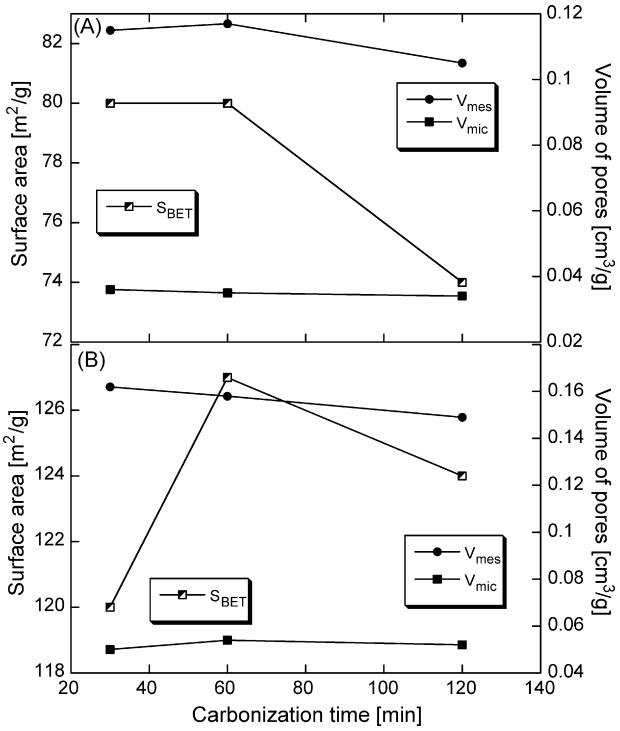

Fig. 2. Trends in the structural parameters with an increase in the carbonization time for the samples pyrolyzed at 650 °C (A) and at 950 °C (B).

The addition of oil has a noticeable effect on the yields of materials (Table 1), which substantially decreased after modifications. As expected, this is caused by the contribution of oil to the initial materials and its decomposition/volatilization during pyrolysis. That effect of oil is also seen in the ash content, which, with an increase in the pyrolysis temperature, increased from about 76% to 85%. The higher carbonization temperature and longer time of carbonization are, less carbonaceous phase is present in our materials. With an increase in the intensity of the pyrolysis, a decrease in the yield is observed which implies differences in the surface features of the samples obtained. The yield of the carbonaceous phase derived in a separate experiment using carbonization of waste oil was about 4%.

To evaluate structural parameters, nitrogen adsorption isotherms were measured. The structural parameters calculated from them are collected in Table 2. Generally speaking, the materials have low porosity with the predominant volume of mesopores and surface areas about 130 m^2/g or less. As seen, in comparison with two samples obtained without oil, the addition

Table 2
Structural parameters of adsorbents studied

Sample	S_{BET} (m^2/g)	V_t (cm^3/g)	V_{mic} (cm^3/g)	V_{mes} (cm^3/g)	V_{mic}/V_t (%)
CT-30-650	48	0.281	0.023	0.258	8
CT-30-650ED	55	0.295	0.024	0.258	8
CT-30-950	NP[a]	NP	NP	NP	ND
CT-30-950ED	NP	NP	NP	NP	ND
CTO-30-650	80	0.151	0.036	0.115	23
CTO-30-650ED	28	0.113	0.011	0.102	10
CTO-60-650	80	0.152	0.035	0.117	23
CTO-60-650ED	29	0.125	0.012	0.113	10
CTO-120-650	74	0.139	0.034	0.105	25
CTO-120-650ED	28	0.110	0.012	0.098	11
CTO-30-950	120	0.212	0.050	0.162	24
CTO-30-950ED	91	0.205	0.036	0.145	17
CTO-60-950	127	0.212	0.054	0.158	26
CTO-60-950ED	92	0.185	0.036	0.149	20
CTO-120-950	124	0.201	0.052	0.149	26
CTO-120-950ED	91	0.191	0.037	0.154	19

[a] Nonporous.

of an organic phase significantly increases the surface areas. The CT-30-950 and CTO-30-650 samples are examples. The former sample was nonporous when no oil was used. It is interesting that while the addition of oil increases the volume of micropores of at least 50%, the volume of mesopores is not changed. That increase in the volume of micropores can have its origin in the new carbonaceous phase derived from oil, which is likely deposited on the surface. On the other hand, the decreased volume of mesopores suggests that carbon from oil is located there forming the micropores.

With an increase in the carbonization temperature and time the structural parameters change. The trends in their values are presented in Fig. 2. For the samples obtained at 650 °C (Fig. 2A) the micropore volumes remain constant while a decrease in the volumes of mesopores and surface area is observed with an increase in the pyrolysis time. These results suggest that the carbonaceous phase, which is likely responsible for the majority of microporosity reached its quasi equilibrium state after 30 min carbonization. Small changes in the volumes of mesopores and surface areas are likely caused by changes in the inorganic phase.

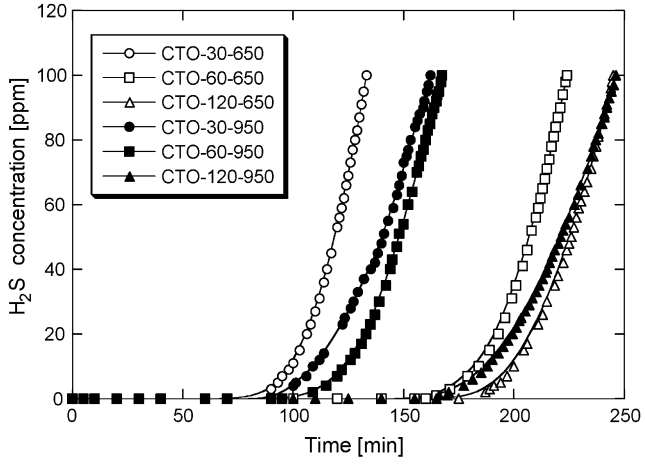

Fig. 3. H_2S breakthrough capacity curves.

These changes seem to be more complete with an increase in the holding time. On the other hand, the structural parameters of the samples obtained at 950 °C are much more dependent on the reaction time (Fig. 2B). Moreover, the maximum values in the surface area and volume of micropores are found for the samples pyrolyzed for 60 min or longer. These changes might be caused by formation of new pores, either in the carbon deposit or in the inorganic phase as a result of the decomposition of an inorganic matter and release of gases and water, which have to find their way out of the solid. These changes are seen as small peaks on DTG curve (Fig. 1). Another aspect is an increase in the degree of carbonization of the carbonaceous phase and solid-state reactions, which are more likely to occur at 950 °C than at 650 °C.

The mentioned above parameters of the porous structure should have their effects on the performance of adsorbents as the desulfurization media. The H_2S breakthrough curves from which the breakthrough capacities were calculated (Table 3) are collected in Fig. 3. As seen, the breakthrough times increase with an increase in the carbonization temperature and time. The most dramatic effects of an increase in the capacity are seen between the CTO-30-650/CTO-60-650 and CTO-60-950/CTO-120-950 pairs of samples. For both pairs of samples twice longer time needed for H_2S to be detected in the outlet gas is observed. This suggests that the most dramatic changes in the structure and

Table 3
H_2S breakthrough capacity results (at 100 ppm) and bed densities for samples run in dry conditions

Sample	Breakthrough capacity (mg/g)	Breakthrough capacity (mg/cm^3)	Bed density (g/cm^3)
CT-30-650	20.2	10.3	0.51
CT-30-950	1.5	0.9	0.60
CTO-30-650	12.1	6.2	0.51
CTO-60-650	19.5	10.5	0.53
CTO-120-650	20.6	11.5	0.55
CTO-30-950	13.8	7.5	0.55
CTO-60-950	14.5	7.8	0.54
CTO-120-950	22.2	11.1	0.51

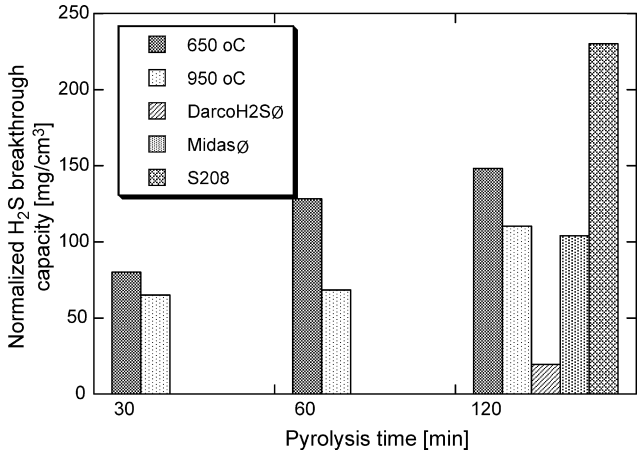

Fig. 4. Comparison of the normalized capacity.

chemistry occur when pyrolysis time increases from 30 to 60 min for the samples obtained at 650 °C and from 60 to 120 min for the samples obtained at 950 °C.

Table 3 lists the breakthrough capacities calculated in mg per unit mass of the adsorbent and in milligram per unit volume of the adsorbent. The latter values are important from the point of view of the real-life performance of materials since the adsorber volume is always one of the limiting factors of the technology applied. Comparison with the capacity obtained when no oil modification was carried out indicates the beneficial aspects of our treatment, especially for the samples carbonized at 950 °C. Although the capacity measured on CTO-30-650 is smaller than that on the unmodified sample, an increase in the carbonization time shows its positive effects on the performance. The high capacity of the CT-30-650 sample was attributed to the chemical reactivity of its inorganic surface on which sulfides could be formed [34]. An addition of carbon could deactivate those centers not only by their physical blocking but also by formation of carbonates or carbides during pyrolysis. If this is true, an increase in the carbonization time of this sample must result in changes in the mechanism of adsorption since the metal oxide-based centers should have a similar level of "deactivation" by CO_2 regardless of the carbonization time. It is likely that the small pores developed in the carbon deposit became active in trapping hydrogen sulfide and then in its oxidation to sulfur [35], not to sulfides. Of course, it can only happen provided that enough oxygen is chemisorbed on the surface or there are other oxidants, such as chromium (VI), which are able to accept electrons from sulfur.

One of the factors contributing to the dramatic increase in the desulfurization performance of the oil modified samples obtained at 950 °C must be that discussed above increase in the porosity in comparison with the unmodified sample. It is interesting that although the surface area and pore volumes increase with an increase in the holding time of pyrolysis between 30 and 60 min, this increase has no effect on the desulfurization capacity. On the other hand, long holding time leads to the very reactive surface. This suggests, that longer heat treatment, besides changes in the porosity, results also in changes in surface chemistry, which alter the mechanism of surface reactions.

Based on the H_2S breakthrough test, the samples obtained at 650 °C outperform samples obtained at 950 °C with an exception of CTO-120-950. To evaluate the dependence of surface activity on the pyrolysis conditions, the capacity was normalized per unit pore volume and the results are presented in Fig. 4. As seen, the surface desulfurization activities of the low temperature samples is much higher than those of the high-temperature pyrolyzed samples. Moreover, while for the latter samples the surface activities seem to be less pyrolysis-time-dependent, a significant effect of pyrolysis time is revealed for the former materials. Their activities dramatically increase when the treatment time is longer. To investigate this effect, the surface chemistry has to be analyzed. For comparison the capacities reported previously on catalytic (DarcoH$_2$S® and Midas®) and virgin coconut shell based (S208) carbons are included in Fig. 4. While catalytic carbons are deactivated in the presence of CO_2 and exhibit lower capacity then those on our materials, the capacity of S208 is still higher owing to its 10 times higher volume of micropores than those in our materials [30]. Nevertheless, the results obtained on our adsorbents are very promising from the point of view of their applications for desulfurization of digester gas.

One of the methods used to evaluate surface chemistry of samples is the measurement of the surface pH value. That pH, when in the basic range, was found as an extremely important factor for the desulfurization process [35]. Basic species, besides a direct reaction with hydrogen sulfide can also provide

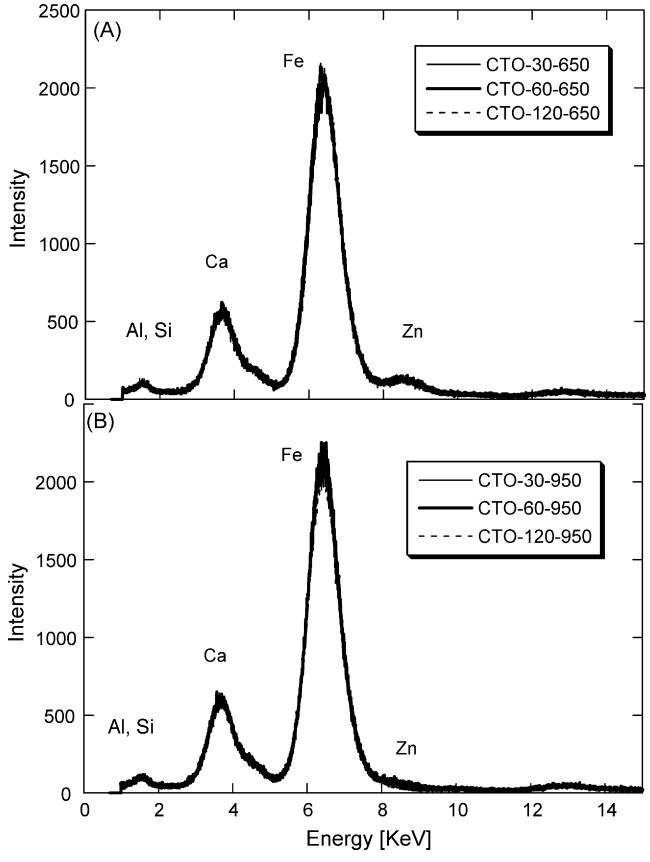

Fig. 5. XRF spectra for the initial and exhausted adsorbents.

Table 4
Content of catalytically important elements (%)

Sample	C	N	H	Ca	Fe	Zn
CTO-30-650	21.1	2.1	0.55	3.85	5.31	0.11
CTO-120-650	21.5	2.0	0.55	4.01	5.44	0.11
CTO-120-650ED	20.4	2.1	0.04	3.98	5.18	0.11
CTO-30-950	19.7	0.9	0.15	4.43	6.11	0.10
CTO-60-950	19.2	0.8	0.26	4.46	6.08	0.07

the proper environment for hydrogen sulfide dissociation when water is present [35,36]. In our case, even though only a small amount of physically adsorbed water could exist on the surface, that water, when located in small pores can be important for hydrogen sulfide oxidation to sulfur. In fact, without the pre-humidification, it is reasonable to assume [37] that adsorbed moisture from the atmosphere can exist only in micropores. After hydrogen sulfide adsorption, the pH can change, when water-soluble salts or sulfuric acid are the products of surface reactions [35]. When sulfur or insoluble sulfides are formed, the pH should be more or less constant. The pH values for our materials before and after H_2S adsorption are listed in Table 1. All materials are very basic. An origin of that basicity is certainly in high calcium content as seen on XRF spectra for the initial and exhausted samples (Fig. 5). It is interesting that the addition of oil slightly increases the surface pH. This might be due to the free valences of graphene layers, which are responsible for the basicity of activated carbons [38] or organic nitrogen incorporated within carbon phase [39,40]. Moreover, an increase in the carbonization temperature increases the pH, which can be also linked to the carbon phase and its increased level or aromatization. After H_2S adsorption, practically no changes in the pH are found which indicates formation of sulfur and/or sulfides on the surface of our materials. Although the samples obtained without oil are included here only for comparison, the one unit increase in the pH of the sample could be caused by changes in the chemical environment of soluble metals salts which after the H_2S exposure are converted into insoluble sulfides.

The contents of carbon, nitrogen, hydrogen, calcium, iron and zinc in our materials are listed in Table 4. The amounts of those elements were analyzed because they are considered as important for surface oxidation of hydrogen sulfide [35]. It should be mentioned here that according to the manufacturer in the initial sludge there are about 1.3% of zinc, 5% of iron, 0.3% of nickel, 0.25% of copper, 0.1% of tin, 0.5% of chromium and 1.3% of cadmium. After carbonization the content of iron and calcium are high which should have a positive effect on hydrogen sulfide oxidation. On the other hand, the content of zinc is very small. This is caused by low temperature of zinc compound decomposition and evaporation of this metal during pyrolysis at, at least, 650 °C [12]. The content of organic carbon in our materials is about 20% and it slightly decreases with the pyrolysis temperature or time, as expected. It is interesting that the samples pyrolyzed at 650 °C have a relatively high content of organic nitrogen. Since after pyrolysis at 950 °C twice less nitrogen is present, it is likely that those compounds are organic amines, which may affect both, the basicity of samples and their performance as hydrogen sulfide adsorbents/catalysts [39]. The apparent discrepancies in the ash and carbon content can be explained by a low accuracy of the ash estimation method and decomposition of inorganic compounds which may contribute to mass changes and CO_2 content (f carbonates are present).

More details about surface chemistry of our materials can be obtained from X-ray diffraction experiments. The examples of the obtained diffraction patterns are compared in Fig. 6. As seen, higher pyrolysis temperature and longer time lead to higher amounts of crystallographic phases seen as sharp peaks. Those phases are formed as a result of solid-state reactions [25–28]. The variations in the pyrolysis time affect the surface of the low temperature pyrolyzed samples to greater extent than those for the high-temperature pyrolyzed samples. This must have an effect on the performance of adsorbents, which was also more pyrolysis-time-dependent for the 650 °C pyrolyzed samples than for those pyrolyzed at 950 °C. The analysis of XRD spectra revealed the predominant crystallographic phases present in our materials. They are listed in Table 5. Besides silica, low temperature pyrolyzed samples have some alkali metal sulfates and rare alloy type compounds made of iron, nickel and chromium. With an increase in the pyrolysis temperature aluminium starts to be engaged and other nonstoichiometric sulfides or oxides are detected. Since no new sulfur compounds are found for the exhausted samples, it supports our hypothesis about amorphous sulfur present on its surface. The high capacity of the samples obtained at 650 °C can be related to the catalytic effect

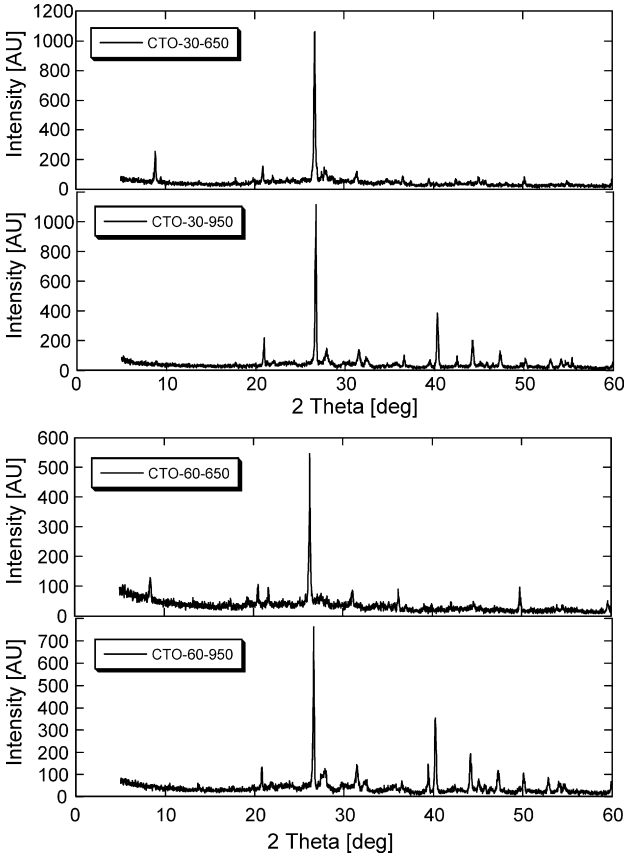

Fig. 6. Examples of XRD diffraction patterns.

Table 5
Crystallographic phases detected using XRD analysis

Sample				
CTO-30-650	SiO_2	$LiNaSO_4$		
CTO-60-650	SiO_2	NiFeCr		$Zn_2Fe(CN)_6$
CTO-120-650	SiO_2		FeNi-kamacite	
CTO-120-650ED	SiO_2	$LiNaSO_4$		
CTO-30-950	SiO_2	AlNi	Cu_5FeS_4	$Bi_{1.09}Ca_{0.91}O_{2.55}$
CTO-60-950	SiO_2	$(Al,Fe)_3$ (PO_4,VO_4)		$Bi_{1.09}Ca_{0.91}O_{2.55}$

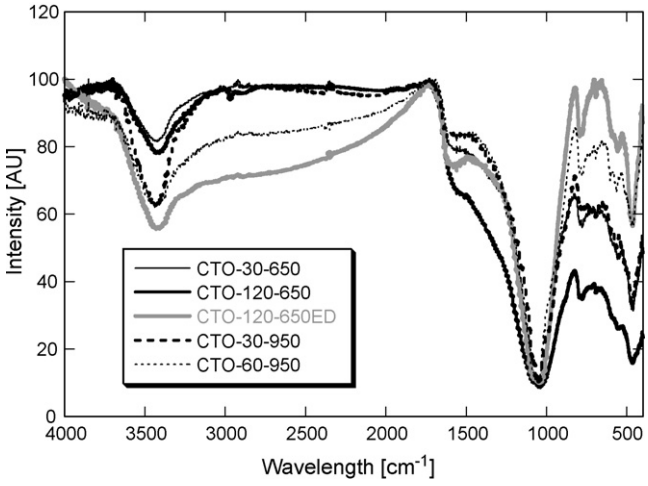

Fig. 7. FTIR spectra.

of iron and/or nickel compounds well-dispersed on the surface. Although reduced iron or carbides can be present in our materials pyrolyzed at high-temperature as a result of reducing atmosphere and the presence of carbon, they were not detected using XRD. Their surface dispersion can be very high.

The changes in the chemistry are also clearly seen on the FTIR spectra collected in Fig. 7. The peaks between 800 and 1200 cm^{-1} represent Si–O(Si) and Si–O(Al) vibration from tetrahedral or alumino- and silico-oxygen bridges in aluminosilicates [41]. The presence of OH^- is represented by a broad peak between 3200 and 3600 cm^{-1}. It is interesting that more OH– is detected for samples obtained at 950 °C than for those at 650 °C. Nevertheless exposure of CTO-120-650 to hydrogen sulfide significantly increases the intensity of OH– band. This can be linked to formation of water as a by-product in the reaction of H_2S oxidation [35]. Other important differences between samples are found in the wavelength between 1100 and 1700 cm^{-1}. The sample obtained by carbonization at 650 °C for 2 h shows the vibrations characteristic for aromatic amines [42]. This is in agreement with the higher level of aromatization of carbon materials when the carbonization process is more intensive. Moreover, the band at about 1600 cm^{-1} is related to the presence of aliphatic amines and amides. They are more pronounced for low temperature pyrolyzed samples owing to their relatively low decomposition temperature [39,40]. This is consistent with the high content of organic nitrogen in those samples. A very broad band at 2200 cm^{-1} can be linked to CN^- groups, which were also detected using XRD analysis. The absorption between 2000 and 2500 cm^{-1} can be also linked to nitriles, imines an

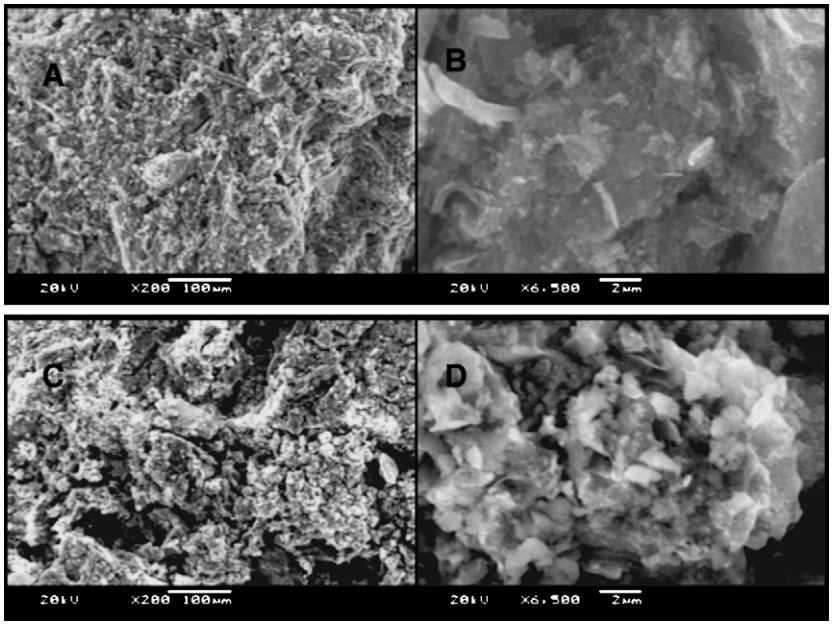

Fig. 8. SEM micrographs for CTO-60-650 (A and B) and CTO-60-950 (C and D).

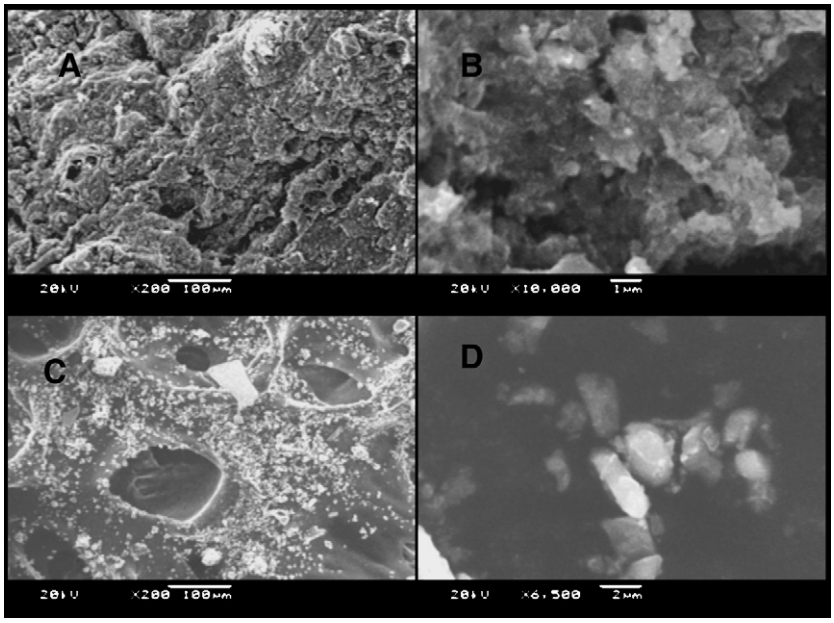

Fig. 9. SEM micrographs for CTO-30-650 (A and B) and CTO-120-650 (C and D).

isocynamides [42], which in fact should be incorporated to carbon at high carbonization temperatures [39]. At this stage of our study we cannot explain the strong absorption between 2000 and 3300 cm^{-1} for the exhausted CTO-120-650ED. The only difference in the chemistry of this sample compare to the CTO-120 is the presence of sulfur and, likely, carbonates.

The changes in chemistry are accompanied by changes in the texture of our materials. Comparison of the surfaces of CTO-60-650 and CTO-60-950 is presented in Fig. 8. SEM micrographs show that an increase in the carbonization temperature has a dramatic effect on the textural properties. On the surface of the sample carbonized at higher temperature larger pores are seen and in higher magnification it looks like the recrystallization occurred during pyrolysis, which is not noticed for the low temperature pyrolyzed counterpart. The surface of the latter sample looks smoother than that for CTO-60-950. On the other hand, longer carbonization time for the samples obtained at 650 °C results in formation of a smoother surface with large round cavities/macropores, which look like they were formed during melting of some sample components (Fig. 9). On that surface, the well-dispersed crystals are seen. Difference in the color intensity suggests different chemistry of this well-dispersed phase. These observed increases in the degrees of surface heterogeneity have likely their effects on the measured increased capacities for desulfurization and increased porosities. After removal of hydrogen sulfide, the CTO-120-650ED surface looks totally different than that before the removal and large agglomerates of amorphous sulfur are seen (Fig. 9). This indicates that all surface is active in the desulfurization process.

The surface reaction products, when deposited on the surface, should block the existing porosity. The structural parameters of the exhausted samples are listed in Table 3. It has to be pointed out here that these parameters are overestimated, and thus the effect of oxidation products on the porosity is underestimated, since the visual analysis of the outgassing tube (even though the outgassing was done at 100 °C) shows deposition of elemental sulfur on cooled tube walls. Moreover, based on the SEM micrograph presented in Fig. 10, the materials are exhausted when all porosity is totally blocked by sulfur. Thus the porosity analysis can actually show the activity of very small pores in our materials from which to remove sulfur more energy is needed. As seen from Table 3, for the samples after H_2S adsorption from digester gas and high vacuum outgassing, the surface areas decrease up to 70% with a similar decrease in the volume of micropores.

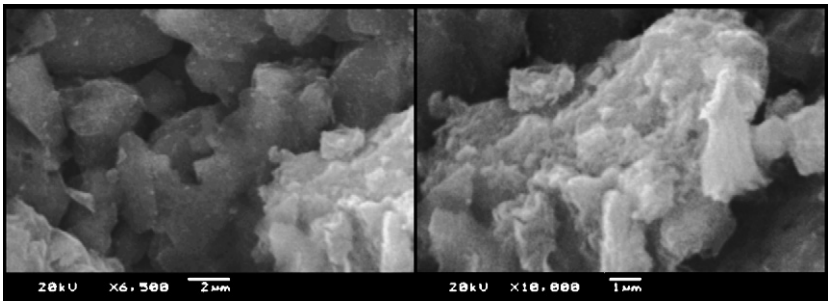

Fig. 10. SEM micrographs of the CTO-120-650 sample after removal of hydrogen sulfide.

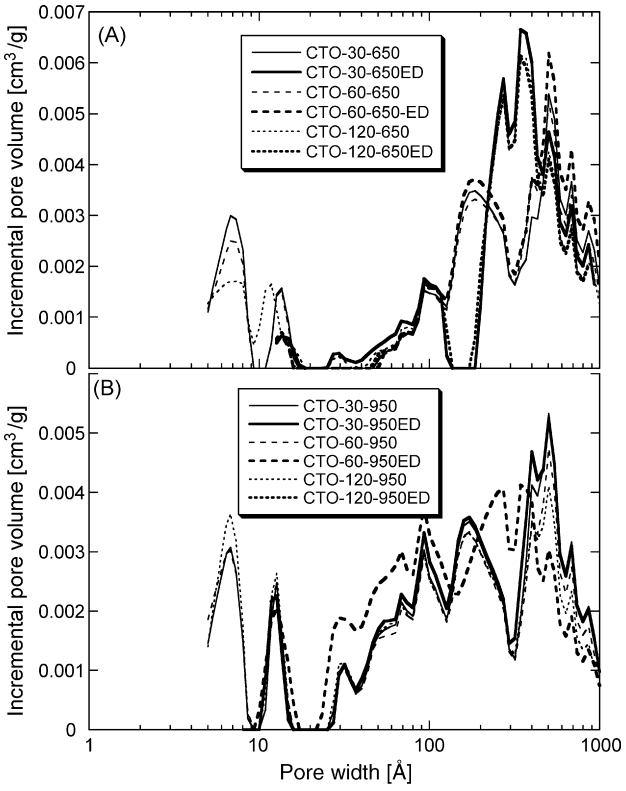

Fig. 11. Pore size distributions for the samples pyrolyzed at 650 °C (A) and at 950 °C (B).

A slight decrease in the volume of mesopores is noticed only for the samples obtained at 950 °C, which may be related to their small sizes. As indicated above, only in those pores water can be present [37], which might have a beneficial effect on adsorption of hydrogen sulfide. These pores can have their origin predominantly in the carbon phase. Moreover, the active basic nitrogen centers have the high probability to be incorporated there [39,40]. The activity of the whole surface (meso- and macropores as revealed by SEM analysis) can be the result of catalytic activation of the inorganic phase via solid-state reactions. As indicated by X-ray diffraction analysis the chemistry of the inorganic phase changes with pyrolysis conditions.

Details of changes in the porosity are seen on the pore size distributions presented in Fig. 11. As indicated above, small pores, smaller than 10 Å are totally blocked by the oxidation products for both series of samples. For the samples obtained at 650 °C the products are also deposited in micropores smaller than 20 Å (Fig. 11A). This might be related to the higher capacity found on these materials than on their high-temperature pyrolyzed counterparts. Another apparent difference is formation of a new pore volume in the range of mesopores, likely within a sulfur deposit seen on SEM micrograph for the exhausted sample (Fig. 10). Although the new pores are also formed on the surface of the exhausted samples obtained at 950 °C, their pore sizes seem to be more heterogeneous and range from 20 to 1000 Å, especially for samples exposed to longer holding time. This supports our hypothesis about the differences in the mechanism of sulfur deposition between the two categories of samples, governed by their surface chemistries. Moreover, it is interesting that pores between 10 and 20 Å are not affected in the samples pyrolyzed at 950 °C.

Comparison of the PSDs for the initial samples pyrolyzed at 650 and 950 °C shows a consistent effect of temperature, mentioned above, on the activation of pore forming agents, which seem to be responsible for the development of pores with sizes between 20 and 100 Å. These pores are present in a significant volume in the samples pyrolyzed at high-temperature.

The presence of sulfur on the surface of our materials can be also seen on DTG curves measured in nitrogen. The comparison of the initial and exhausted samples is presented in Fig. 12. The peaks at temperature lower than 120 °C represent the removal physically adsorbed water, confirming the hypothesis about its presence and thus about its effect on the surface reactions. As previously, we assign the peak between 200 and 400 °C revealed on all curves for the exhausted samples to the removal of elemental sulfur from the large pores, Its intensity should depend on the capacity. For the samples obtained at 650 °C an additional peaks are present between 400 and 650 °C and heterogeneity of the oxidation products (number of peaks) increases with an increase in the carbonization time and thus desulfurization capacity. The first peak centered at about 480 °C may represent iron sulfate or elemental sulfur deposited in very small pores, like those in carbon deposit discussed above. The second, centered at 600 °C may be assigned to zinc sulfate [42]. In those samples small amount of zinc is still present. Based on the intensity of those peaks and taking into account the content of iron and zinc in the adsorbents, the yield of sulfates, if formed, would be very

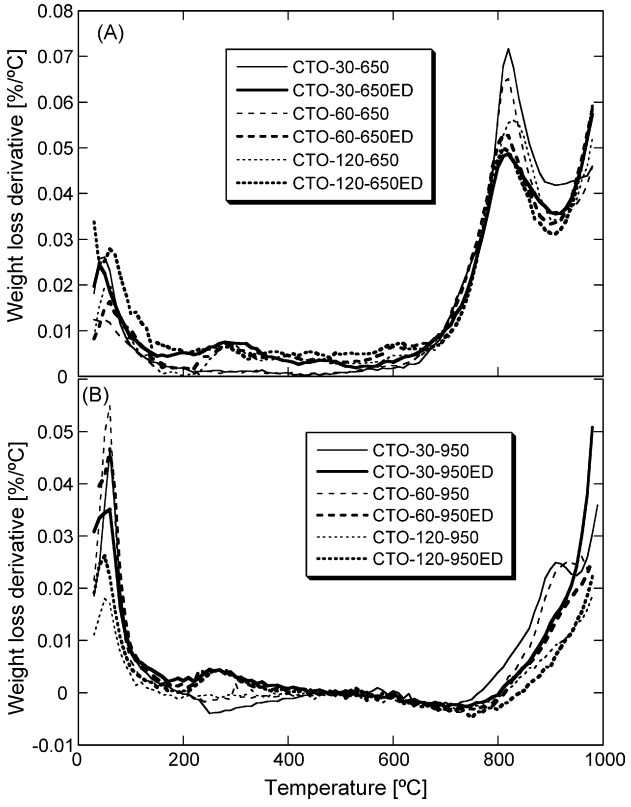

Fig. 12. DTG curves in nitrogen for the samples pyrolyzed at 650 °C (A) and at 950 °C (B).

Table 6
Balance of sulfur species based on the weight loss evaluated from TA and on the H_2S breakthrough capacity results

Sample	$\Delta W_{200-400}$ (%)	$\Delta W_{400-650}$ (%)	H_2S adsorbed (%)
CTO-30-650ED	1.14	0.08	1.2
CTO-60-650ED	1.00	1.09	1.9
CTO-120-650ED	1.09	1.02	1.9
CTO-30-950ED	0.53	0	1.3
CTO-60-950ED	0.46	0	1.4
CTO-120-950ED	0.37	0	2.1

small. Therefore, it is more likely that the broad peak at 480 °C represents sulfur removed from very small pores of carbonaceous phase, since those pores looked as being completely filled with sulfur on PSDs. Its broadness depends on the heterogeneity of pore sizes. The thermal desorption process seems to be continuous. Supporting for the hypothesis of formation of elemental sulfur as the predominant species is the balance of sulfur listed in Table 6. As seen, total weight loss between 200 and 650 °C resembles the amount of sulfur deposited in the surface. These results also support mentioned above hypothesis about the changes in the mechanism of desulfurization on the materials pyrolyzed at 650 °C on which a carbonaceous phase is present. This phase definitely promotes formation of sulfur and sulfides are not the important products of surface reactions. It is likely that metal centers, which were engaged in formation of sulfides (calcium, zinc and iron based) when carbon phase was not present [34], are converted into carbonates during carbonization and thus their reaction activity vanishes. This carbonaceous phase must also act as some reservoir for oxygen to promote the oxidation process. In fact it should be more active in oxygen retention owing to its lower level of carbonization. Chromium species, if in the oxidized form, can also contribute to the oxidation process. Moreover, the nitrogen compounds present on the surface of carbons were indicated as oxygen activators [43].

DTG curves for the samples obtained at 950 °C exposed to hydrogen sulfide show only one peak between 200 and 400 °C which is attributed to the removal of elemental sulfur (Fig. 12B). Since weight loss in this temperature range is much smaller than that expected assuming that only sulfur polymers are formed on the surface (Table 6), the only plausible explanation is formation of sulfides, which decompose at temperature higher than 1000 °C. This was also hypothesized for sewage sludge derived materials [14,15]. In fact, on the DTG curves a decrease in the weight loss is noticed at temperature higher than 800 °C, which suggests that metals engaged in carbonates, which should decompose at this temperature range might be involved in formation of sulfides. Moreover, for these samples an increase in the weight was also revealed for the initial and exhausted samples in the range between 200–400 °C and 600–800 °C even though the experiments were run in UHP purity nitrogen after careful calibration and standardization for pure carbon materials (no increase in the weight for pure graphite or carbon black was measured). As before, the only plausible explanation is either formation of nitrides via carboreduction [44,45] or reactivity of the surface with the decomposition products. Since the mass increase between 600 and 800 °C is similar for the initial and exhausted samples, the incorporation of sulfur is excluded. Although the mass decrease for the initial samples can compensate slightly for the amount of elemental sulfur desorbed between 200 and 400 °C, the balance of sulfur cannot be reached.

4. Conclusions

The results presented in this paper show a significant effect of pyrolysis conditions on the development of structural and catalytic properties of new, metal sludge/waste oil based adsorbents. These materials show increased catalytic activity for removal of hydrogen sulfide from digester gas, compared to only metal sludge derived adsorbents. On their surface hydrogen sulfide is predominantly oxidized to elemental sulfur. The catalysts for this process seem to be nitrogen-containing basic groups highly dispersed on the surface of the carbonaceous phase and/or new inorganic phase containing iron and zinc. The waste oil precursor provides that active carbonaceous phase which is also responsible for development of micropores. Moreover, it contributes to formation of new active surface chemistry either by supplying carbon element or by reducing environment for reactions involving the inorganic compounds. The long holding time and high-temperature of pyrolysis stabilize both, organic and inorganic, phases. These phases undergo aromatization, carbonization, thermal decomposition, incorporation of nitrogen and undefined solid-state reactions. These processes not only change surface chemistry but also significantly affect the porosity and texture of the adsorbents.

Acknowledgements

This work was supported by NYSERDA agreement #9405 (RF CUNY #55771-0001) and PSC CUNY grant #67284-00-36. Partial support was obtained from The National Basic Research Program of China (2005CB221203) and the Program fro New Century Excellent Talents in Universities of China (No. NCET-04-0274). The authors are grateful to Ms. Anna Kleyman, Dr. Mykola Seredych for experimental help.

References

[1] Biosolids regeneration, use, and disposal in the United States: EPA530-R-99-009, U.S. EPA, Washington, DC, September 1999, www.epa.gov.
[2] B.H. Jones, US Patent 4,781,994 (1988).
[3] P.C. Chiang, J.H. You, Can. J. Chem. Eng. 65 (1987) 922–926.
[4] F.M. Lewis, US Patent 4,122,036 (1977).
[5] J. Sutherland, US Patent 3,998,757 (1976).
[6] R.D. Nickerson, H.C. Messman, US Patent 3,887,461 (1975).
[7] H. Abe, T. Kondoh, H. Fukuda, M. Takahashi, T. Aoyama, M. Miyake, US Patent 5,338,462 (1994).
[8] N.R. Khalili, H. Arastoopour, L.K. Walhof, US Patent 6,030,922 (2000).
[9] G.Q. Lu, J.C.F. Low, C.Y. Liu, A.C. Lau, Fuel 74 (1995) 44–3450.
[10] A. Bagreev, T.J. Bandosz, Ind. Eng. Chem. Res. 40 (2001) 3502–3510.
[11] G.Q. Lu, D.D. Lau, Gas Sep. Purif. 10 (1996) 103–108.
[12] A. Bagreev, T.J. Bandosz, D.C. Locke, Carbon 39 (2001) 1971–1977.
[13] A. Bagreev, T.J.J. Bandosz, Colloid Interf. Sci. 252 (2002) 188–194.

[14] A. Bagreev, S. Bashkova, D.C. Locke,.T.J. Bandosz, Environ. Sci. Technol. 35 (2001) 1537–1543.
[15] A. Bagreev, T.J. Bandosz, Environ. Sci. Technol. 38 (2004) 345–351.
[16] M.J. Martin, A. Artola, M. Dolors Balaguer, M. Rigola, Chem. Eng. J. 94 (2002) 231–239.
[17] F.S. Zang, H.J. Toh, Hazard. Mater. B 101 (2003) 323–327.
[18] F.S. Zang, J.O. Nriangu, H.J. Itoh, Photochem. Photobiol. A: Chem. 167 (2004) 223–228.
[19] S. Rio, C. Faur-Brasquet, L. Le Coq, P. Courcoux, P. Le Cloirec, Chemosphere 58 (2005) 423–437.
[20] S. Rio, C. Faur-Brasquet, L. Le Coq, P. Le Cloirec, Environ. Sci. Technol. 39 (2005) 4249–4257.
[21] A. Ansari, A. Bagreev, T.J. Bandosz, Carbon 43 (2005) 359–367.
[22] A. Ansari, T.J. Bandosz, Environ. Sci. Technol. 39 (2005) 6217–6222.
[23] E. Sioukri, T.J. Bandosz, Environ. Sci. Technol. 39 (2005) 6225–6230.
[24] M.J. Martin, E. Serra, A. Ros, M.D. Balaguer, M. Rigola, Carbon 42 (2004) 1389–1394.
[25] A. Ros, M.A. Montes-Moran, E. Fuente, D.M. Nevskaia, M.J. Marin, Environ. Sci. Technol. 40 (2006) 3102–3110.
[26] T.J. Bandosz, K. Block, Ind. Chem. Eng. Res. 45 (2006) 3666–3672.
[27] T.J. Bandosz, K. Block, Environ. Sci. Technol. 40 (2006) 3378–3383.
[28] T.J. Bandosz, K. Block, Appl. Catal. Environ. 67 (2006) 77–85.
[29] M. Seredych, T.J. Bandosz, Energy Fuels 21 (2007) 858–866.
[30] M. Seredych, T.J. Bandosz, Ind. Chem. Eng. Res. 45 (2006) 3658–3665.
[31] M.M. Dubinin, in: P.L. Walker (Ed.), Chemistry and Physics of Carbon, vol. 2, M. Dekker, New York, 1966, pp. 51–120.
[32] Ch.M. Lastoskie, K.E. Gubbins, N. Quirke, J. Phys. Chem. 97 (1993) 4786–4796.
[33] J.P. Olivier, J. Porous Mater. 2 (1995) 9–14.
[34] W. Yuan, T.J. Bandosz, Fuel, in press.
[35] A. Bagreev, T.J. Bandosz, Ind. Chem. Eng. Res. 44 (2005) 530–538; T.J. Bandosz, in: T.J. Bandosz (Ed.), Activated Carbon Surfaces in Environmental Remediation, Elsevier, Oxford, 2006, pp. 231–292.
[36] A. Primavera, A. Trovarelli, P. Andreussi, G. Dolcetti, Appl. Catal. A: Gen. 173 (1998) 185–192.
[37] C.L. McCallum, T.J. Bandosz, S.C. McGrother, E.A. Muller, K.E. Gubbins, Langmuir 15 (1999) 533–544.
[38] C.A. Leon y Leon, L.R. Radovic, in: P.A. Thrower (Ed.), Chemistry and Physics of Carbon, vol. 24, M. Dekker, New York, 1992, pp. 213–310.
[39] F. Adib, A. Bagreev, T.J. Bandosz, Langmuir 16 (2000) 1980–1986.
[40] J.R. Pels, F. Kapteijn, J.A. Moulijn, Q. Zhu, K.M. Thomas, Carbon 33 (1995) 1641–1650.
[41] M. Rivera-Garza, M.T. Olguin, I. Garcia-Sosa, D. Alcantra, G. Rodriguez-Fuentes, Silver supported on natural Mexican zeolite as an antibacterial material, Micropor. Mesopor. Mater. 39 (2000) 431–444.
[42] R.C. West (Ed.), Handbook of Chemistry and Physics, 67th ed., Academic Press, Boca Raton, FL, 1986.
[43] B. Strohr, H.P. Boehm, R. Schlogl, Carbon 26 (1991) 707–711.
[44] O. Yamamoto, M. Ishida, Y. Saitoh, T. Sasamoto, S. Shimada, Int. J. Inorg. Mater. 3 (2001) 715–719.
[45] R. Koc, S. Kaza, J. Eur. Ceram. Soc. 18 (1998) 1471–1477.